

(NASA-CR-194108) PHOTOCHEMICAL  
MODELLING OF VENUS CLOUDS USING  
PIONEER VENUS DATA Final Report  
(Harvard Univ.) 22 p

N94-10823

Unclas

G3/91 0182921

GRANT  
1N-91-CR  
0.97.  
182921  
NAG2-264

## Introduction

In order to understand the evolution of water on Venus, we must know the hydrogen escape flux as a function of the tropospheric water abundance. We have studied the connection between total stratospheric hydrogen and exobase hydrogen available to non-thermal escape processes and examined the details of the photochemical trap for water at the Venus cloud tops. Our immediate goal is to calculate the stratospheric water abundance as a function of the tropospheric water abundance.

The ratio of stratospheric water to tropospheric water is of order  $10^{-2}$  (von Zahn and Moroz, 1984), while the ratio of stratospheric  $\text{SO}_2$  to tropospheric  $\text{SO}_2$  apparently varies from  $10^{-4}$  to  $10^{-2}$  (Esposito, 1984; von Zahn and Moroz, 1984). Photochemical production of  $\text{H}_2\text{SO}_4$  acts as a sink for both water and sulfur and is capable of keeping stratospheric abundances low if a proper balance exists between the tropospheric abundances. If production of  $\text{H}_2\text{SO}_4$  were the only sink for  $\text{H}_2\text{O}$  and  $\text{SO}_2$ , the excess in tropospheric abundance of one over the other would reach the stratosphere, and the functional dependence of stratospheric  $\text{H}_2\text{O}$  on tropospheric  $\text{H}_2\text{O}$  would be linear near the present state. On Venus, however, sulfuric acid condenses at cloud top temperatures and the resulting aerosols can absorb additional water of hydration. This complicates the water budget, increasing the efficiency of sulfur as a sink for water. We have investigated the balance between tropospheric  $\text{H}_2\text{O}$  and  $\text{SO}_2$  and how delicate the balance is.

## Procedure

For this investigation we have used a one dimensional photochemical model to investigate the atmosphere of Venus between the cloud tops and the exobase (Yatteau, 1983). Results from the upper atmosphere model are

used as upper boundary conditions for the cloud model, which calculates composition between 47 km and 70 km. Chemistry of carbon-, oxygen-, hydrogen-, chlorine-, and sulfur-bearing species is calculated following the work of Yung and Demore (1983) and Yatteau (1983). The list of reactions considered in the photochemical model, together with their rate coefficients, is given in Table 1. Settling of  $H_2SO_4$  aerosols is modelled using a constant settling velocity appropriate for mode 2 aerosols (Knollenberg and Hunten, 1980). Hydration of  $H_2SO_4$  aerosols is calculated using equilibrium at local temperature and humidity. Lower boundary densities of  $H_2O$  and  $SO_2$  are treated as adjustable parameters whose range is constrained by observation. Lower boundary densities for radical species are set to zero, since photochemical production is negligible at the cloud base, and lower boundary mixing ratios for long-lived species are set to spectroscopically determined values. Eddy diffusivity is assumed to follow a downward extrapolation of von Zahn et al. (1980) profile with a lower bound as an adjustable parameter.

### Results

Figure 1 shows typical dayside mixing ratio profiles of important hydrogen-bearing species between the cloud top region and the exobase. HCl and  $H_2O$  are efficiently converted to atomic H above 100 km, which establishes a direct relationship between total stratospheric hydrogen and exobase H.

Supply of  $H_2O$  to the stratosphere is controlled by the photochemical trap near the cloud tops. We have performed a series of calculations for 2 sets of tropospheric  $SO_2$  and  $H_2O$  abundances which yield stratospheric mixing ratios consistent with observation. The  $SO_2$  mixing ratio at 47 km is set to 10 ppm and 40 ppm in the two sets of calculations. The mode 2

particles identified by Knollenberg and Hunten (1980) from the particle size spectrometer data are most likely to be sulfuric acid droplets and they dominate the mass loading in the upper cloud.

Our model calculates more  $\text{H}_2\text{SO}_4$  in the upper cloud than is consistent with simple settling of mode 2 particles at their most likely settling velocity of  $0.03 \text{ cms}^{-1}$ . Figure 2 shows mixing ratio profiles for  $\text{H}_2\text{SO}_4$  corresponding to settling velocities of  $0.03 \text{ cms}^{-1}$  and  $0.06 \text{ cms}^{-1}$  for an  $\text{SO}_2$  mixing ratio of 10 ppm at 47 km; it also shows the mixing ratio profile of  $\text{H}_2\text{SO}_4$  corresponding to the inferred mass loading of mode 2 particles from Knollenberg and Hunten (1980). Figure 3 shows the same profile for an  $\text{SO}_2$  mixing ratio of 40 ppm at 47 km. The discrepancy between the model and observations probably reflects oversimplification in the aerosol model, although the sounder probe may have entered a subsiding region.

Our model calculates aerosol hydration states at the low end of the range inferred from observed indices of refraction, suggesting that the model contains too little water. But higher water abundances are not consistent with low  $\text{SO}_2$  in the cloud region. Figure 4 shows altitude profiles of aerosol hydration state for 2 values of tropospheric  $\text{SO}_2$ .

We have calculated the dependence of stratospheric  $\text{H}_2\text{O}$  mixing ratio on tropospheric  $\text{H}_2\text{O}$  mixing ratio for 40 ppm  $\text{SO}_2$ . Figure 5 shows the  $\text{H}_2\text{O}$  mixing ratio at 70 km as a function of the  $\text{H}_2\text{O}$  mixing ratio at 47 km. The effect of aerosol hydration is to delay penetration of the photochemical trap by  $\text{H}_2\text{O}$ .

Recent reports of variations in stratospheric  $\text{SO}_2$  at 70 km (Esposito, 1984) have prompted us to investigate controls on stratospheric  $\text{SO}_2$  with our model. Since sulfur and hydrogen are so intimately linked, we have also considered associated changes in hydrogen.

We have calculated profiles of  $\text{SO}_2$  and  $\text{H}_2\text{O}$  for different values of eddy diffusivity. We find that  $\text{SO}_2$  varies dramatically, but that  $\text{H}_2\text{O}$  varies less or not at all. Figure 5 shows  $\text{SO}_2$  mixing ratio profiles for 2 values of minimum eddy diffusivity such that the  $\text{SO}_2$  mixing ratios at 70 km are 1 ppb and 100 ppb, the range reported by Esposito (1984). Corresponding profiles for  $\text{H}_2\text{O}$  are shown in Figure 7. These results show that a factor of 3 change in eddy diffusivity can produce a 2 order of magnitude change in  $\text{SO}_2$  at 70 km while lowering  $\text{H}_2\text{O}$  by only a factor of 4. The same calculations for 10 ppm  $\text{SO}_2$  at 47 km are depicted in Figure 8. There is negligible change in  $\text{H}_2\text{O}$  in the case of 10 ppm  $\text{SO}_2$  at 47 km. Since HCl probably supplies at least half the stratosphere's hydrogen (Yatteau, 1983), we conclude that modest changes in the turbulent mixing rate near the cloud tops can account for the reported changes in stratospheric  $\text{SO}_2$  without substantially altering the hydrogen budget. We expect changes of less than a factor of 2 in upper atmospheric hydrogen associated with reported changes in stratospheric  $\text{SO}_2$ .

#### Discussion

We have used our model to examine timescales for changes in stratospheric  $\text{H}_2\text{O}$  and  $\text{SO}_2$  associated with disturbances to the cloud regions. The photochemical timescale for conversion of  $\text{SO}_2$  to  $\text{H}_2\text{SO}_4$  is of order  $10^8$  sec at 70 km and of order  $2 \times 10^5$  sec at 62 km. The diffusive timescale at 70 km is about  $1-2 \times 10^7$  sec depending on the eddy diffusivity, but in the case of low eddy diffusivity, the diffusive timescale at 62 km is about  $3-5 \times 10^7$  sec. We conclude that both  $\text{SO}_2$  and  $\text{H}_2\text{O}$  at 70 km are diffusively controlled, responding to changes lower down.

Our results show that changes in sulfur at 70 km may be associated with changes in  $\text{H}_2\text{O}$ , but the magnitude of the changes in  $\text{H}_2\text{O}$  depends on

the tropospheric  $\text{SO}_2$  abundance. It may be possible to use observations of  $\text{SO}_2$ ,  $\text{H}_2\text{SO}_4$  haze and upper atmospheric H to distinguish between different processes which could be responsible for observed variation, such as direct injection and enhanced mixing. If higher levels of  $\text{SO}_2$  result from enhanced mixing,  $\text{SO}_2$  and  $\text{H}_2\text{O}$  should change on a timescale of order  $10^7$  sec. In situ production of aerosols at 70 km takes about  $10^8$  sec; upward mixing of aerosols produced at 62 km could occur in  $10^7$  sec. Mixing would initiate  $\text{H}_2\text{SO}_4$  production immediately; direct injection would result in less total haze located at different altitudes occurring at later times if the injected material had an  $\text{H}_2\text{O}/\text{SO}_2$  ratio substantially different from the tropospheric ratio. Associated changes in upper atmospheric H may not be dramatic enough to detect. HCl may supply more than half the stratospheric hydrogen budget, and diffusion would prevent even direct injection of pure  $\text{SO}_2$  at 70 km from eliminating water from the stratosphere.

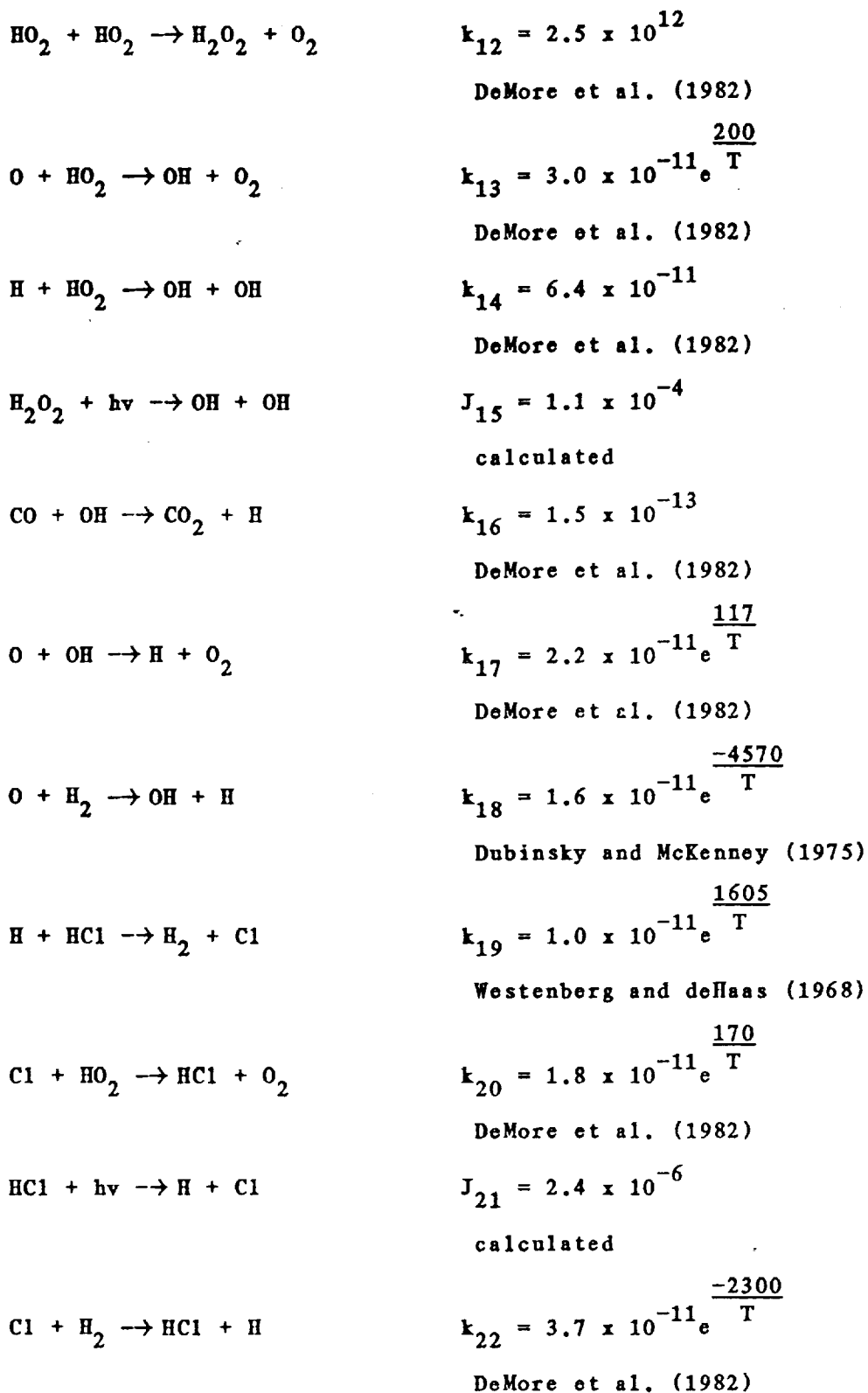
Our major conclusions from this work are the following: 1)  $\text{H}_2\text{O}$  and  $\text{SO}_2$  are mutually limiting if proper tropospheric balance is maintained; 2) changes in tropospheric abundances on the order of 5 ppm are significant; 3) changes in mixing rates near the cloud tops can cause dramatic changes in  $\text{SO}_2$  without causing dramatic changes in  $\text{H}_2\text{O}$ .

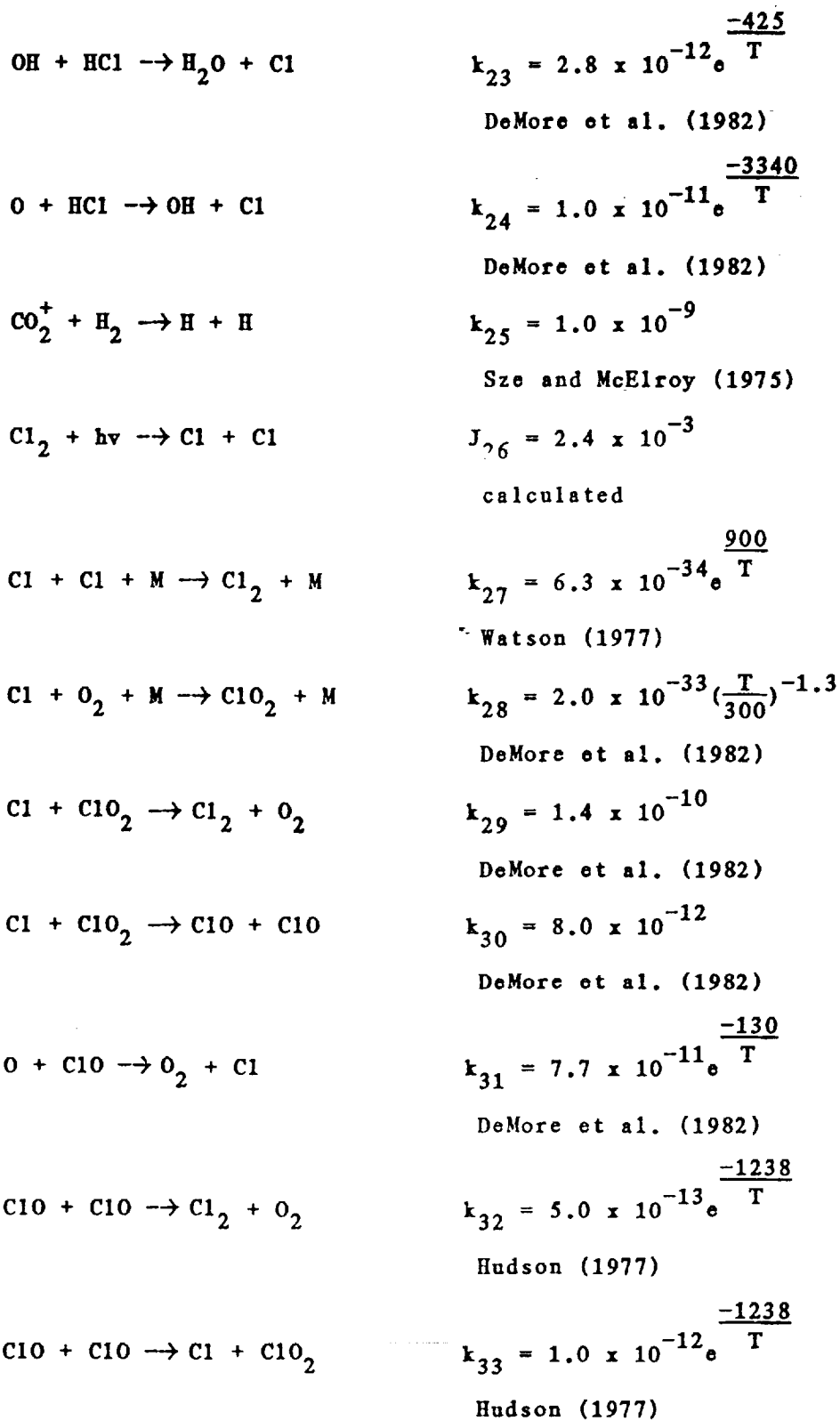
References

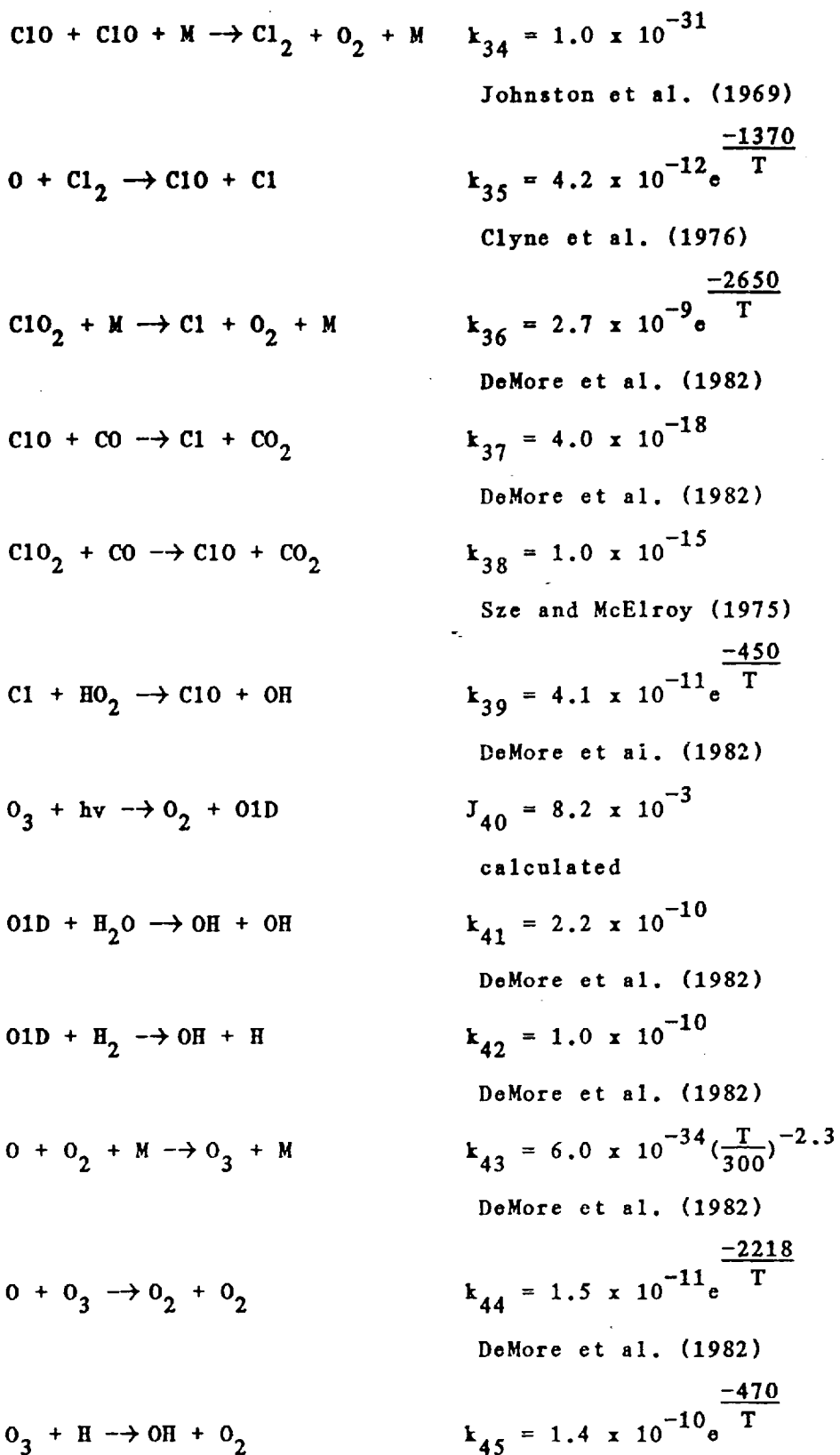
- Esposito, L. W. (1984): Sulfur dioxide: episodic injection shows evidence for action Venus volcanism. Science, 223, 1072.
- Knollenberg, R. G. and D. M. Hunten (1980): The microphysics of the clouds of Venus: results of the Pioneer Venus particle size spectrometer experiment. J.G.R., 85, (A13), 8039.
- von Zahn, U., K. H. Fricke, D. M. Hunten, D. Draukowsky, K. Mauersberger, and A. O. Nier (1980): The upper atmosphere of Venus during morning conditions. J.G.R., 85, (A13), 7829.
- von Zahn, U. and V. I. Moroz (1984): Composition of the Venus atmosphere below 100 km altitude. 25th plenary meeting of COSPAR, June 28-30, 1984, Graz, Austria.
- Yatteau, J. H. (1983): Some issues related to evolution of planetary atmospheres. Ph.D. Thesis, Harvard University.
- Yung, Y. L. and W. B. DeMore (1982): Photochemistry of the stratosphere of Venus: implications for atmospheric evolution. Icarus, 51, 199-247.

Table 1

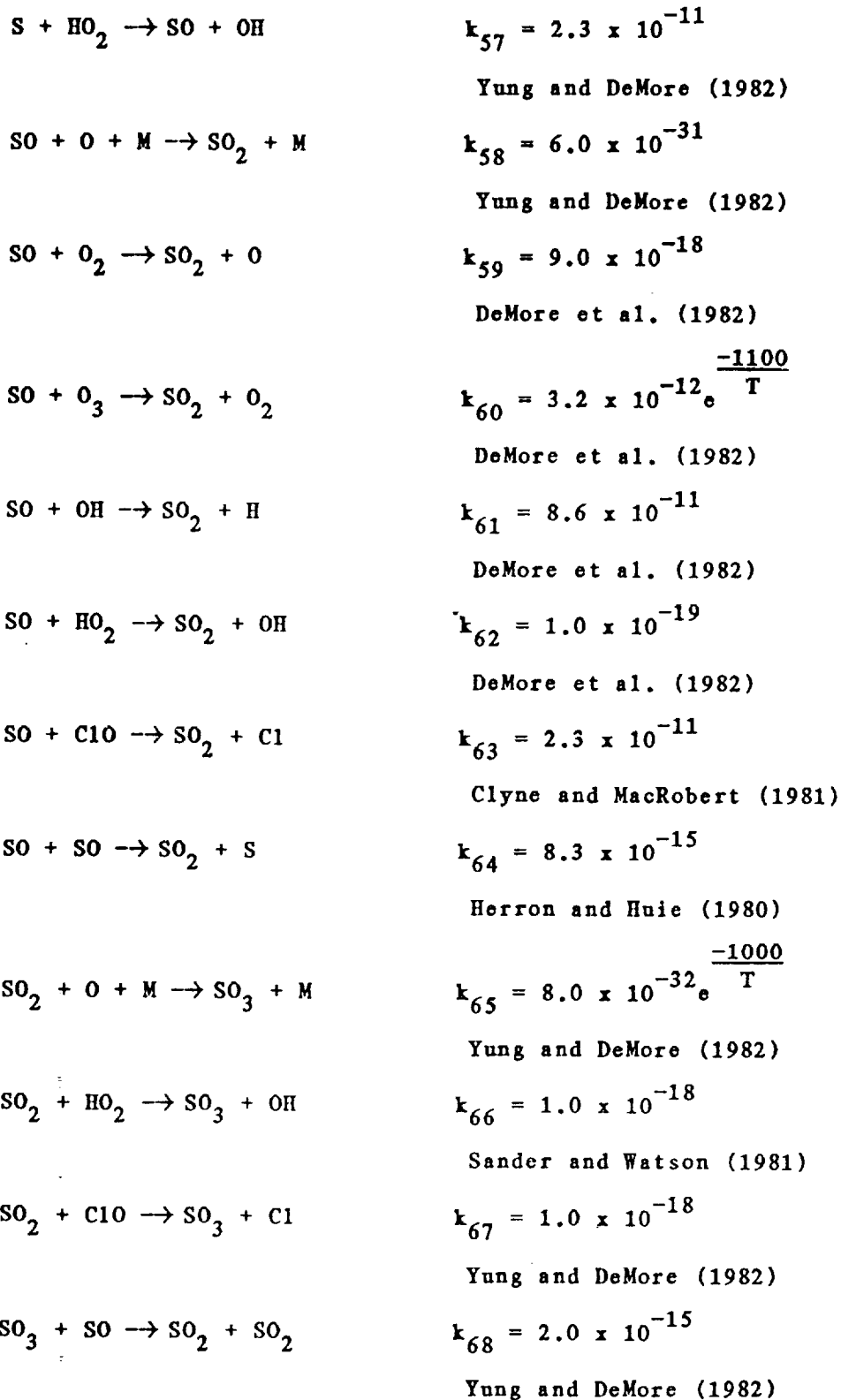
$\text{CO}_2 + h\nu \rightarrow \text{CO} + \text{O}({}^1\text{D})$	$J_1 = 8.8 \times 10^{-7}$ calculated
$\text{O}({}^1\text{D}) + \text{M} \rightarrow \text{O} + \text{M}$	$k_2 = 7.4 \times 10^{-11} e^{\frac{117}{T}}$ DeMore et al. (1982)
$\text{CO} + \text{O} + \text{M} \rightarrow \text{CO}_2 + \text{M}$	$k_3 = 6.5 \times 10^{-33} e^{\frac{-2180}{T}}$ Baulch et al. (1976)
$\text{O} + \text{O} + \text{M} \rightarrow \text{O}_2 + \text{M}$	$k_4 = 4.8 \times 10^{-33} \left(\frac{T}{300}\right)^{-2}$ Campbell and Gray (1973)
$\text{O}_2 + h\nu \rightarrow \text{O} + \text{O}$	$J_5 = 2.2 \times 10^{-6}$ calculated
$\text{H}_2\text{O} + h\nu \rightarrow \text{OH} + \text{H}$	$J_6 = 6.8 \times 10^{-6}$ calculated
$\text{H} + \text{O}_2 + \text{M} \rightarrow \text{HO}_2 + \text{M}$	$k_7 = 5.5 \times 10^{-32} \left(\frac{T}{300}\right)^{-1.4}$ DeMore et al. (1982)
$\text{OH} + \text{HO}_2 \rightarrow \text{H}_2\text{O} + \text{O}_2$	$k_8 = 7.0 \times 10^{-11}$ DeMore et al. (1982)
$\text{H} + \text{HO}_2 \rightarrow \text{H}_2 + \text{O}_2$	$k_9 = 7.0 \times 10^{-12}$ DeMore et al. (1982)
$\text{H} + \text{H} + \text{M} \rightarrow \text{H}_2 + \text{M}$	$k_{10} = 9.2 \times 10^{-33} \left(\frac{T}{300}\right)^{0.802}$ fit to Trainor et al. (1973)
$\text{OH} + \text{H}_2 \rightarrow \text{H}_2\text{O} + \text{H}$	$k_{11} = 6.1 \times 10^{-12} e^{\frac{-2030}{T}}$ DeMore et al. (1982)

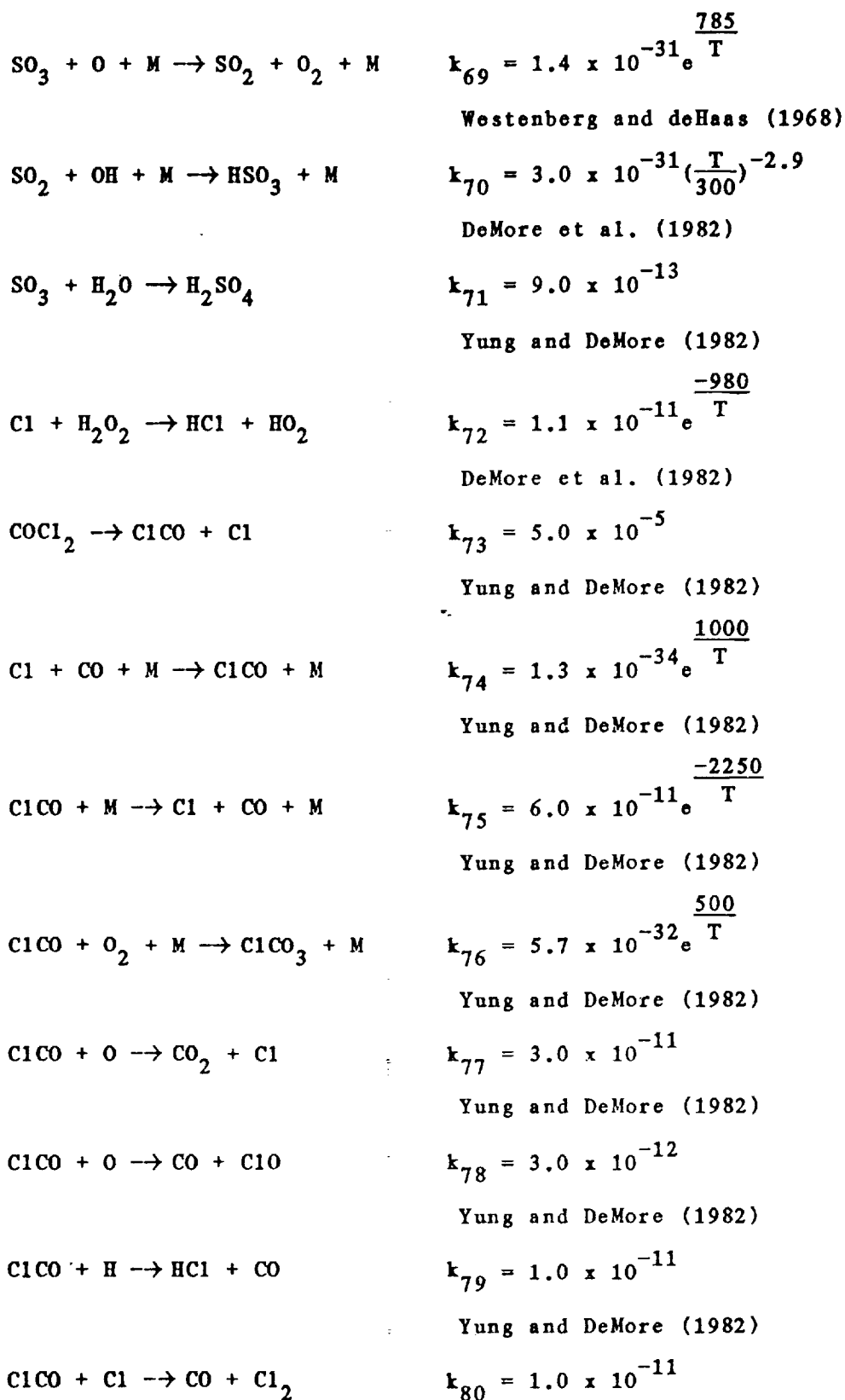






	DeMore et al. (1982)
$O_3 + OH \rightarrow HO_2 + O_2$	$k_{46} = 1.6 \times 10^{-12} e^{\frac{-940}{T}}$
	DeMore et al. (1982)
$O_3 + HO_2 \rightarrow OH + O_2 + O_2$	$k_{47} = 1.4 \times 10^{-14} e^{\frac{-580}{T}}$
	DeMore et al. (1982)
$O_3 + Cl \rightarrow ClO + O_2$	$k_{48} = 2.8 \times 10^{-11} e^{\frac{-257}{T}}$
	DeMore et al. (1982)
$O_3 + ClO \rightarrow ClO_2 + O_2$	$k_{49} = 1.0 \times 10^{-12} e^{\frac{-4000}{T}}$
	DeMore et al. (1982)
$OH + OH \rightarrow H_2O + O$	$k_{50} = 4.2 \times 10^{-12} e^{\frac{-242}{T}}$
	DeMore et al. (1982)
$SO + hv \rightarrow S + O$	$J_{51} = 6.7 \times 10^{-4}$
	calculated
$SO_2 + hv \rightarrow SO + O$	$J_{52} = 1.9 \times 10^{-4}$
	calculated
$S + O_2 \rightarrow SO + O$	$k_{53} = 2.3 \times 10^{-12}$
	DeMore et al. (1982)
$S + CO_2 \rightarrow SO + CO$	$k_{54} = 1.0 \times 10^{-20}$
	Yung and DeMore (1982)
$S + O_3 \rightarrow SO + O_2$	$k_{55} = 1.2 \times 10^{-11}$
	Yung and DeMore (1982)
$S + OH \rightarrow SO + H$	$k_{56} = 6.6 \times 10^{-11}$
	DeMore et al. (1982)





	Yung and DeMore (1982)
$\text{ClCO} + \text{Cl}_2 \rightarrow \text{COCl}_2 + \text{Cl}$	$k_{81} = 6.0 \times 10^{-13} e^{\frac{-1400}{T}}$
	Yung and DeMore (1982)
$\text{ClCO} + \text{ClCO} \rightarrow \text{COCl}_2 + \text{CO}$	$k_{82} = 1.0 \times 10^{-11}$
	Yung and DeMore (1982)
$\text{ClCO}_3 + \text{O} \rightarrow \text{CO}_2 + \text{Cl} + \text{O}_2$	$k_{83} = 1.0 \times 10^{-11}$
	Yung and DeMore (1982)
$\text{ClCO}_3 + \text{Cl} \rightarrow \text{CO}_2 + \text{Cl} + \text{ClO}$	$k_{84} = 1.0 \times 10^{-11}$
	Yung and DeMore (1982)
$\text{ClCO}_3 + \text{H} \rightarrow \text{CO}_2 + \text{Cl} + \text{OH}$	$k_{85} = 1.0 \times 10^{-11}$
	Yung and DeMore (1982)
$\text{H}_2\text{SO}_4 \rightarrow \text{Aerosol}$	condensation
$\text{HSO}_3 \rightarrow \text{Aerosol}$	condensation
$\text{H}_2\text{O} \rightarrow \text{Aerosol}$	hydration
	see text

---

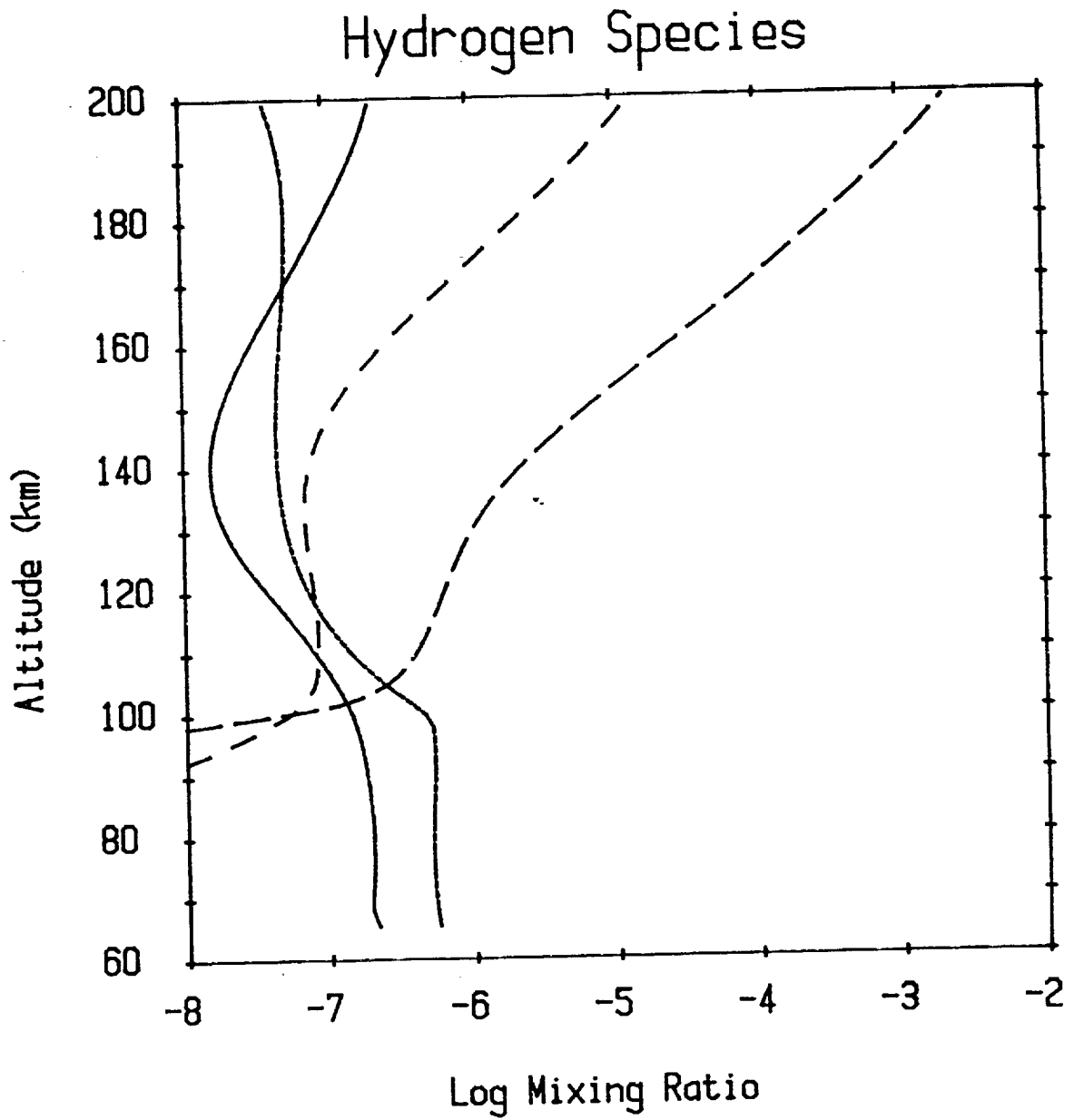


Figure 1

H<sub>2</sub>O (solid line), H<sub>2</sub> (short dashes), H (long dashes), HCl (dash-dot), clouds to exobase.

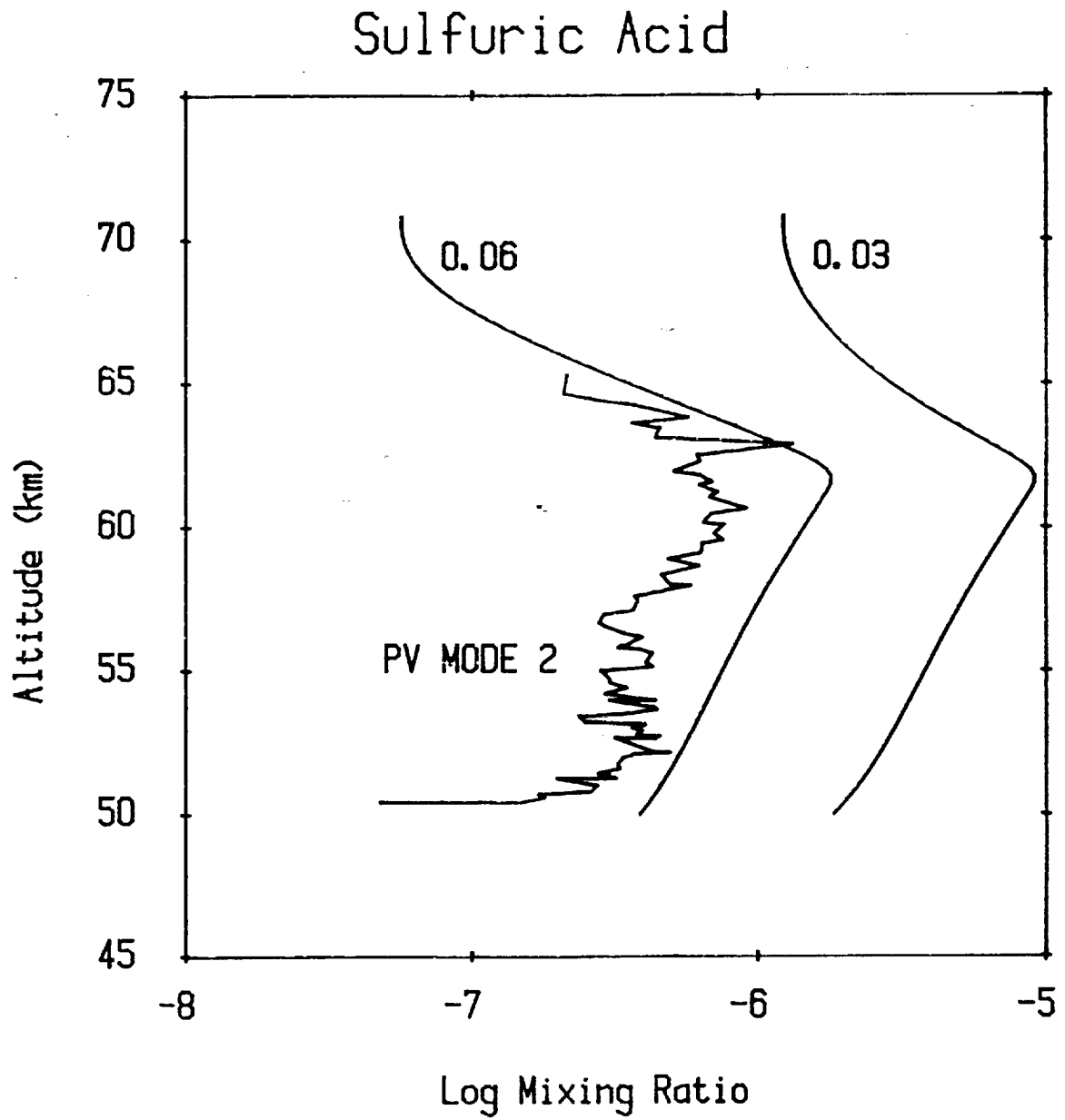


Figure 2

SO<sub>2</sub> = 10 ppm. Settling velocities of 0.03 cm/s and 0.06 cm/s. PV mode 2 also shown.

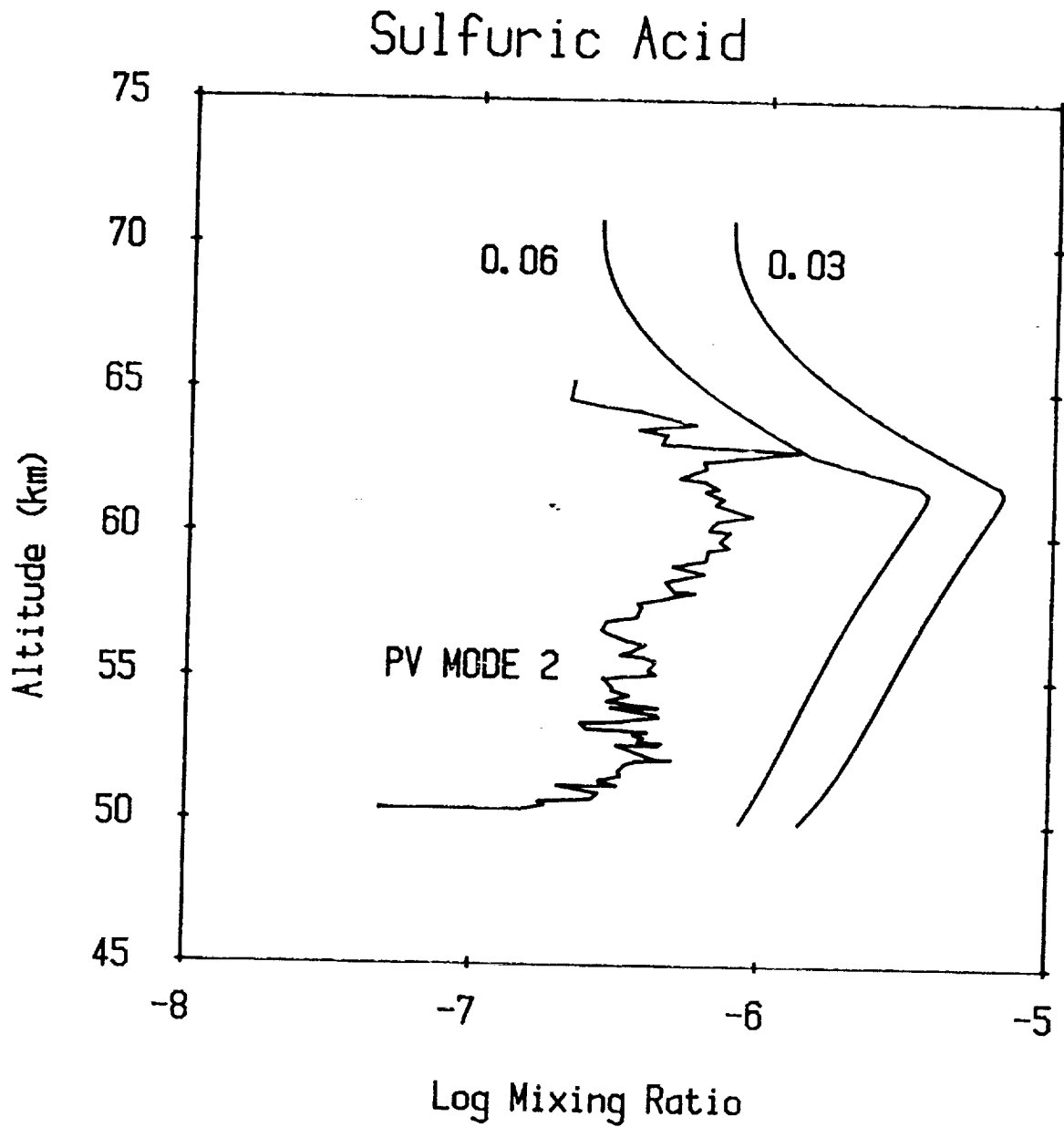


Figure 3

SO<sub>2</sub> = 39 ppm. Settling velocities of 0.03 cm/s and 0.06 cm/s. PV mode 2 also shown.

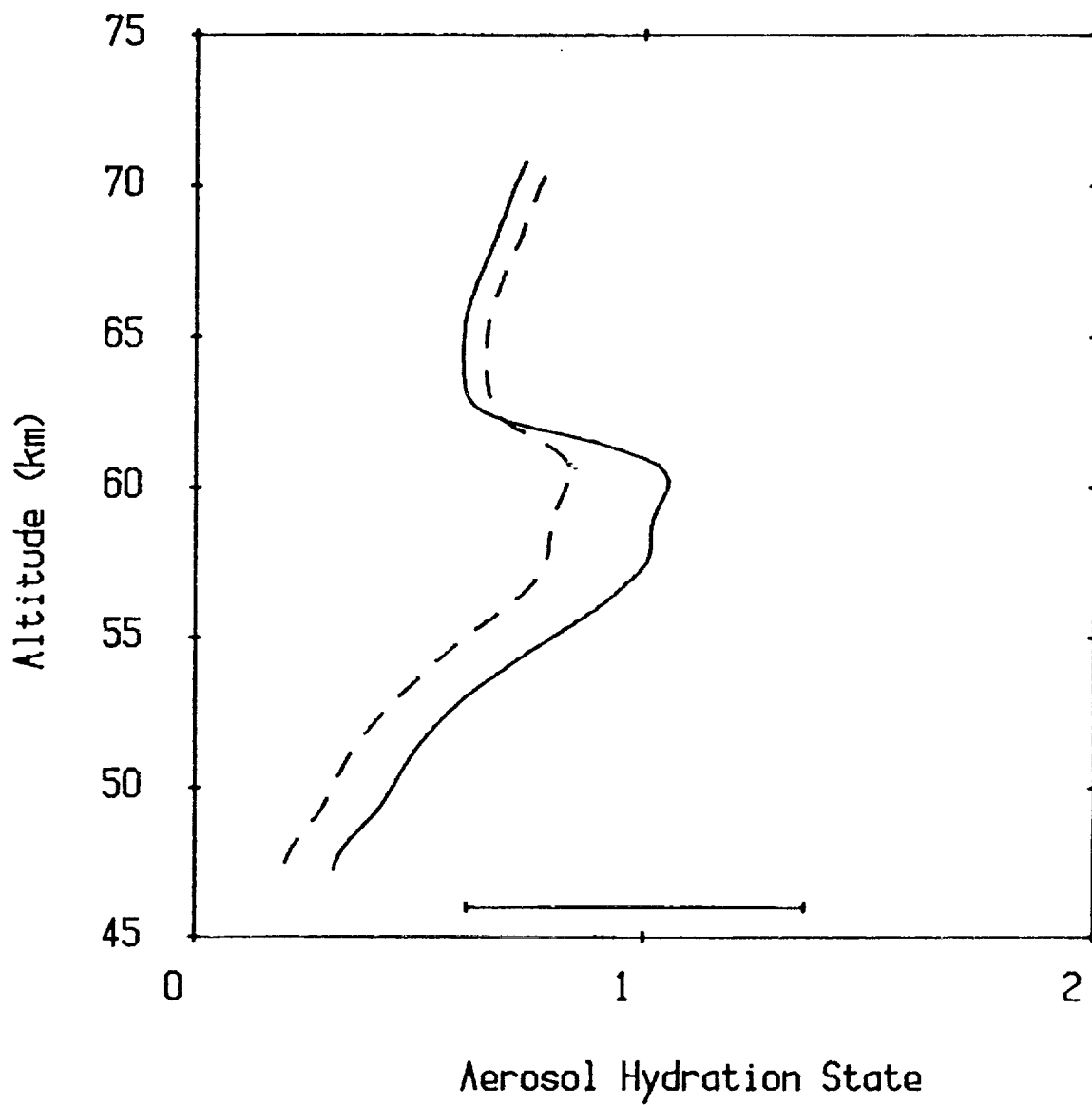


Figure 4

SO2 = 10 ppm (dashed), SO2 = 39 ppm (solid).  
Range inferred from observation also shown.

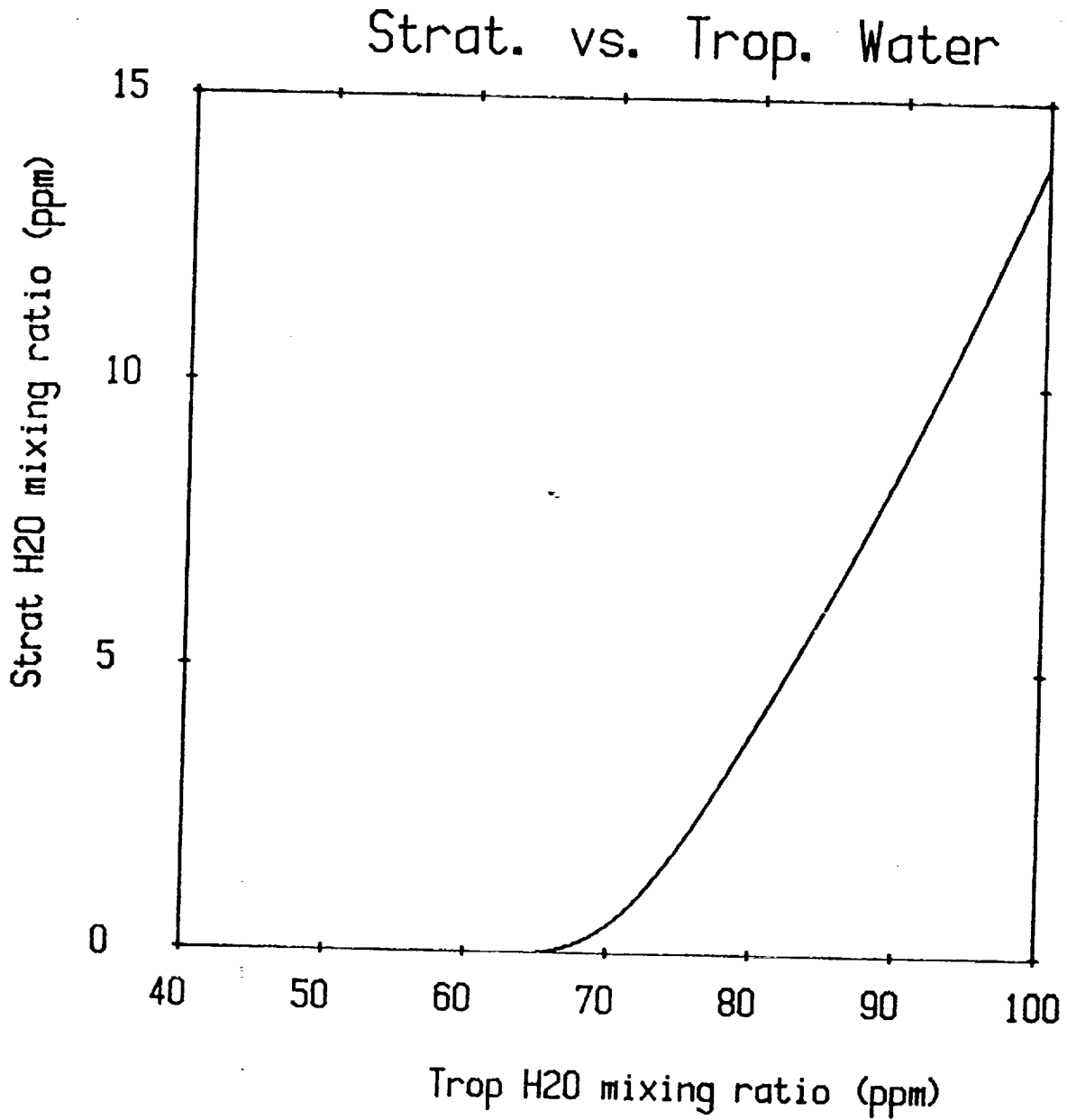


Figure 5

Water vapor mixing ratio at 70 km as a function of water vapor mixing ratio at 47 km.

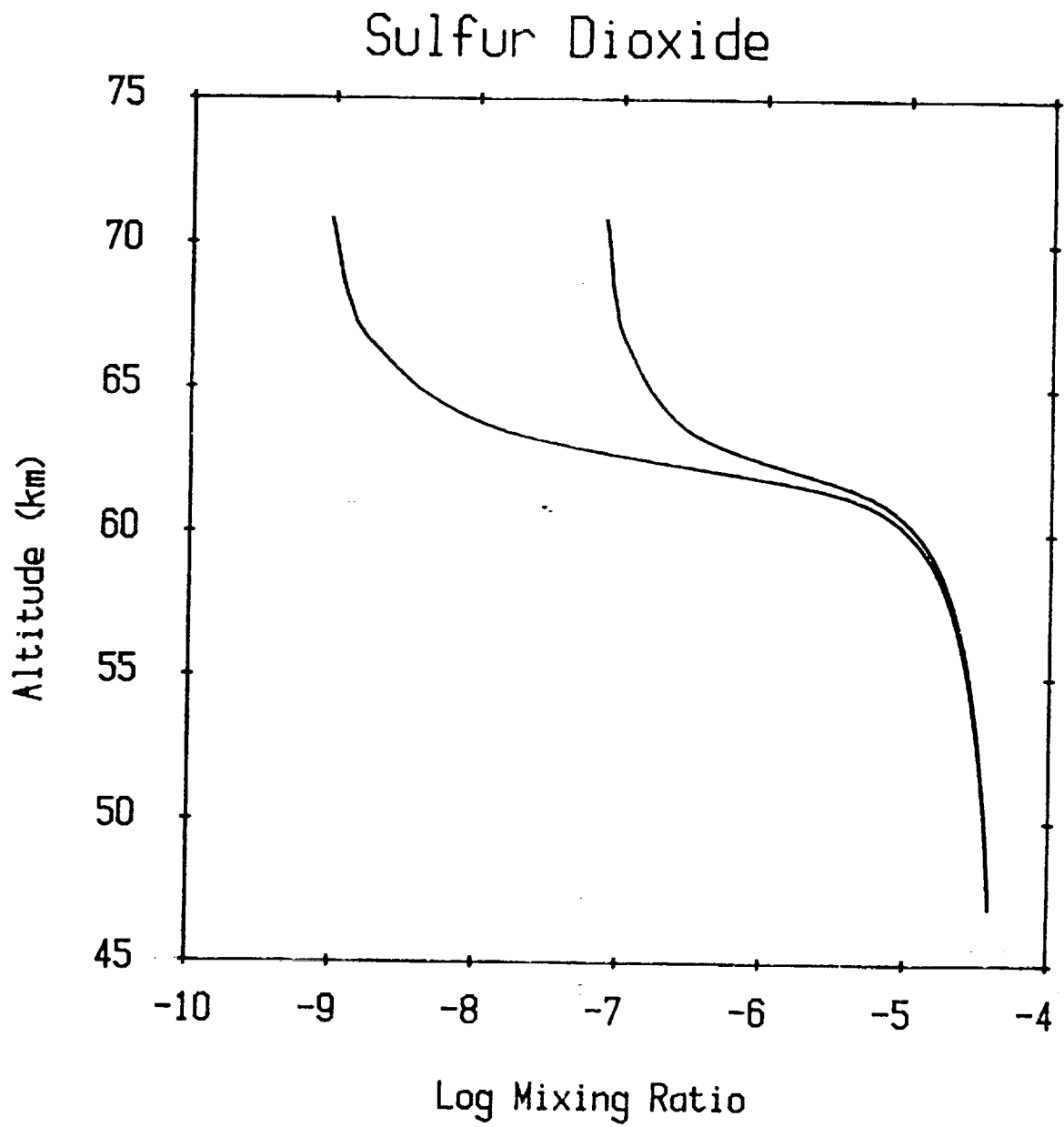


Figure 6

SO<sub>2</sub> for eddy diffusivity =  $6.0E+03$  cm<sup>2</sup>/s and  $2.0E+04$  cm<sup>2</sup>/s.

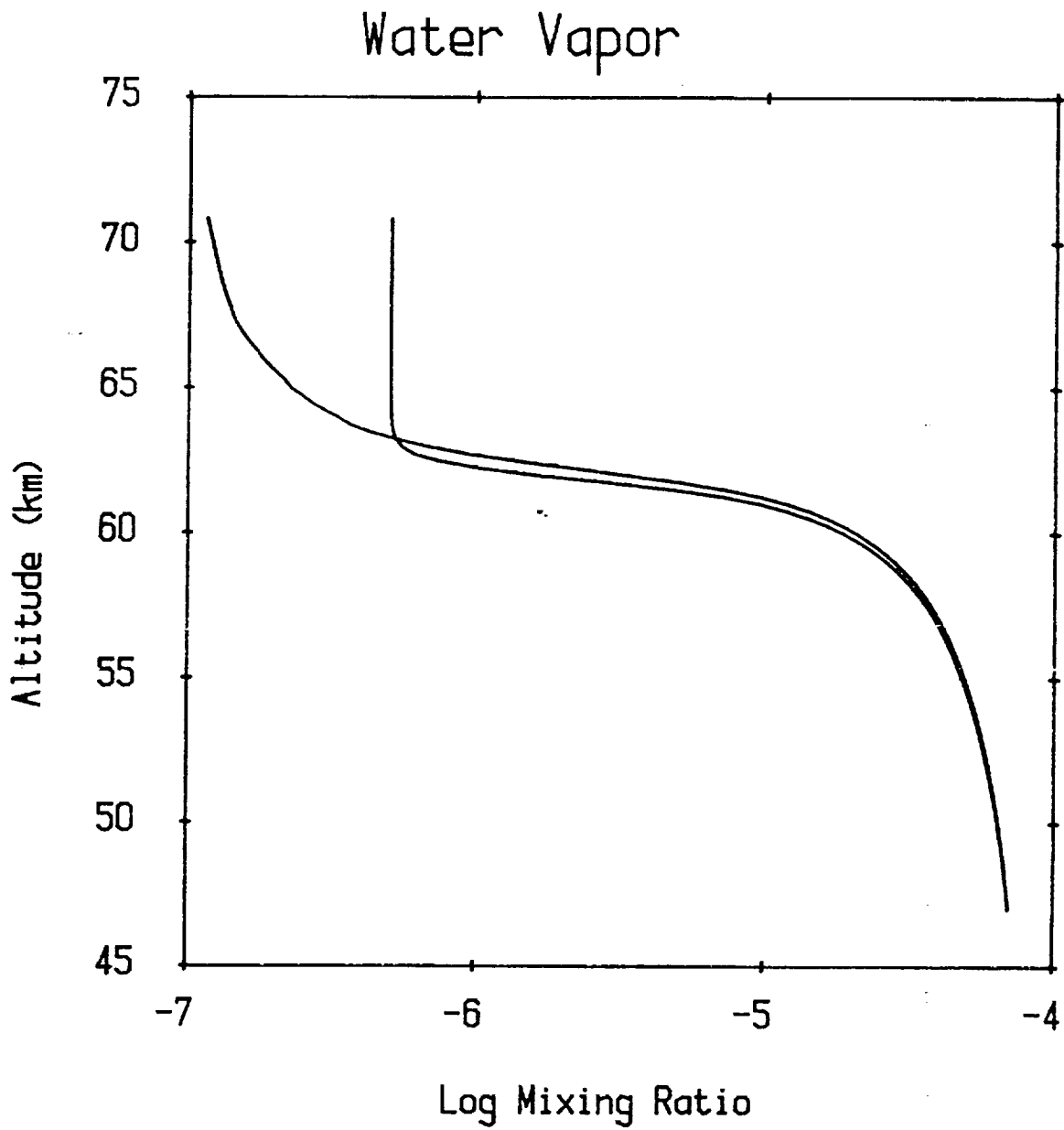


Figure 7

H<sub>2</sub>O for eddy diffusivity =  $6.0E+03$  cm<sup>2</sup>/s and  $2.0E+04$  cm<sup>2</sup>/s

# Sulfur Dioxide

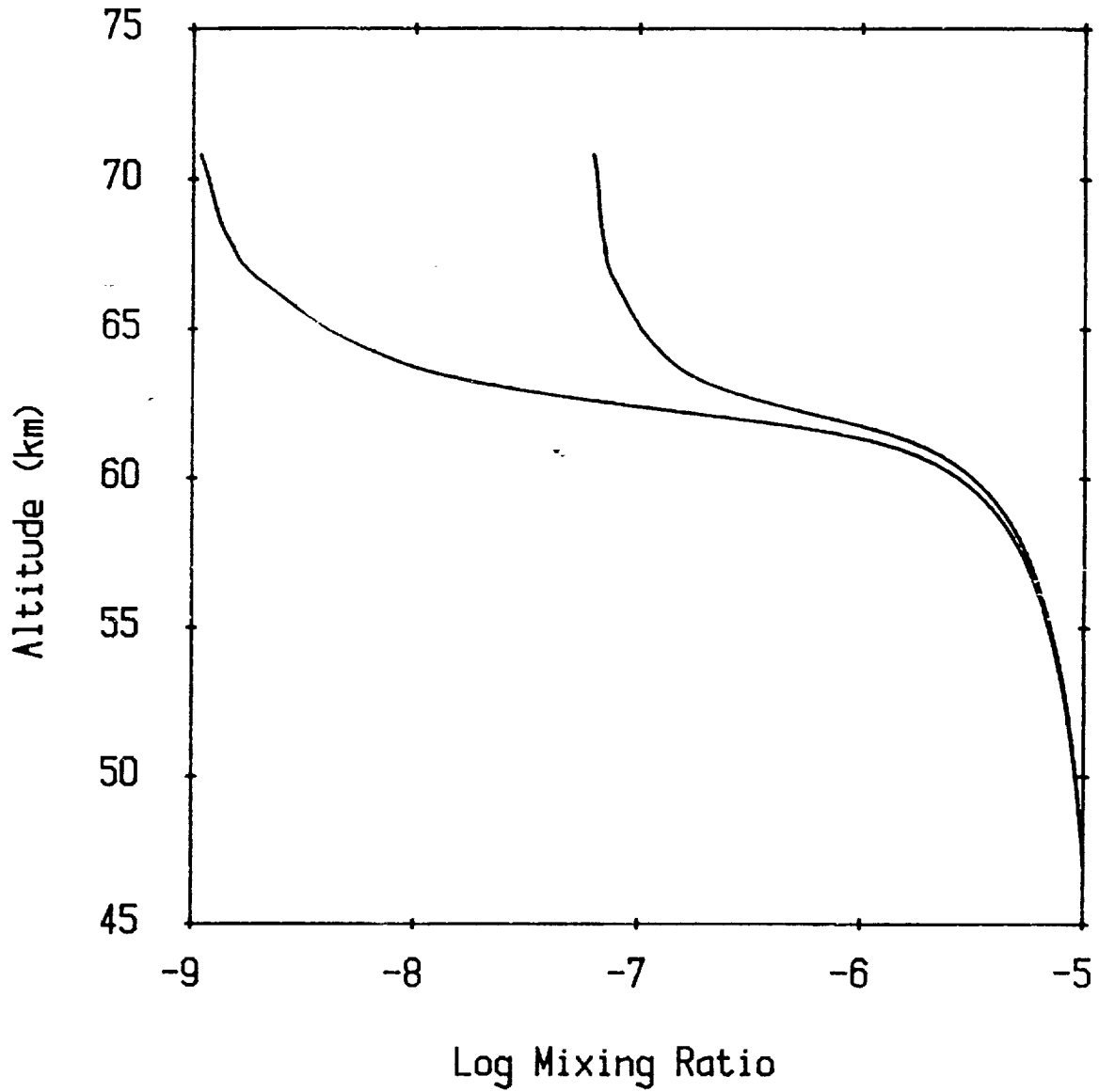


Figure 8

SO<sub>2</sub> for eddy diffusivity =  $9.0E+03$  and  $3.0E+04$ . Water vapor is unchanged.